

RESEARCH ARTICLE

WILEY

Sensitivity of nitrate concentration-discharge patterns to soil nitrate distribution and drainage properties in the vertical dimension

Xiaoli Chen  | Christina L. Tague  | John M. Melack | Arturo A. Keller

Bren School of Environmental Science and Management, University of California at Santa Barbara, Santa Barbara, California

Correspondence

Xiaoli Chen, 5577 San Felipe, Suit 1806, Houston, TX 77057.
Email: haier.cxl@gmail.com

Funding information

National Science Foundation via the Santa Barbara Coastal Long Term Ecological Research Project, Grant/Award Numbers: OCE-1458845, SBC-LTER OCE-1232779; National Science Foundation, Grant/Award Numbers: SBC-LTER OCE-1232779, OCE-1458845

Abstract

We propose a conceptual model that examines the 'variable source area' (VSA) and 'nitrate flushing' hypothesis in the vertical direction, and use this approach to explain nitrate concentration-discharge relationships in a semi-arid watershed. We use an eco-hydrology simulation model (RHESSys) to show that small changes in the vertical distribution of nitrate mass and their interaction with soil hydraulic conductivity can result in abrupt changes in the nitrate concentration-discharge relationship. We show that the estimated concentration-discharge relationship is sensitive to the parameters governing soil vertical nitrate distribution and soil hydraulic conductivity, at both patch scale and watershed scale, where lateral redistribution of water and nitrate is also accounted for. Given heterogeneity in nitrogen inputs, uptake processes, soil drainage and storage processes, substantial variation in parameters that describe rate of changes in vertical distribution of soil nitrate and hydraulic properties is likely both within and between watersheds. Thus, we argue that vertical 'variable source area' processes may be as important as lateral VSA in determining concentration discharge relationships.

KEYWORDS

concentration-discharge relationship, nitrate vertical distribution, variable source area

1 | INTRODUCTION

Nitrate transport from surface and subsurface terrestrial stores to streams is an important nitrate-exporting path. Terrestrial nitrate export impacts water quality and ecosystem function in both terrestrial and coastal ecosystems, reducing nitrate availability for terrestrial plants while increasing nutrient input to downstream ecosystems, impairing water quality and increasing eutrophication (Galloway et al., 2003; Hedin, Armesto, & Johnson, 1995; Page, Reed, Brzezinski, Melack, & Dugan, 2008).

"Concentration-discharge" relationships are often studied to understand mechanisms that lead to nitrate export. For example, Aguilera and Melack (2018a) examined patterns of hysteresis in concentration-discharge relationships and used the direction/rotation of hysteresis pattern to improve the understanding of mechanisms

that deliver materials. Further, concentration-discharge relationships are important given that many downstream impacts are sensitive to nitrate concentration as well as net export. Of particular interest in concentration-discharge relationships are the factors that determine nitrate enrichment (or increasing nitrogen concentration with discharge) or dilution (decreasing nitrogen concentration with discharge) patterns (Godsey, Kirchner, & Clow, 2009; House & Warwick, 1998; Zimmer, Pellerin, Burns, & Petrochenkov, 2019). Previous studies have developed several hypotheses that link concentration-discharge patterns to the interaction between flow paths and nitrate sources. The flushing hypothesis was proposed to explain nitrate concentration peaks during storm events (Hornberger, Bencala, & McKnight, 1994; Ocampo, Oldham, Sivapalan, & Turner, 2006). When soil saturation deficit (the difference between soil porosity and soil water storage) is high, this hypothesis assumes that nitrates accumulate in the upper

layers of the soil. When soil saturation deficit decreases, nitrates in saturated subsurface layers will be washed to streams (Creed et al., 1996). Further development of the flushing hypothesis shows how topographic properties and their influences on variable source area regulate the flushing mechanism and the concentration–discharge relationship (Creed & Band, 1998a, 1998b; Harms & Grimm, 2010). Creed and Band (1998a) emphasize that it is the *rate of expansion* of the variable source area, not the *total* variable source area, that regulates the export of nitrates. Other processes or factors including wild fire (Aguilera & Melack, 2018b; Goodridge et al., 2018; Hanan et al., 2016a), macropore flow (Lohse, Sanderman, & Amundson, 2013), shallow groundwater linkage (Jiang et al., 2015), hillslope hydrologic connectivity (Jencso, McGlynn, Gooseff, Bencala, & Wondzell, 2010) and antecedent soil moisture conditions (Macrae, English, Schiff, & Stone, 2010) also contribute to the regulation of nitrate exports.

Most studies have focused on hydrologic linkages in the horizontal direction, or the impact of the expansion of variable source area on hydrologic linkages in the horizontal direction. A few studies have examined hydrologic linkage in the vertical direction and these studies indicate that soil vertical stratigraphy regulates hydrologic flow paths and water quality dynamics in semi-arid soil (Swarowsky, Dahlgren, & O'Geen, 2012). However, due to substantial uncertainties and lack of details for the semi-arid soils, the implications of the vertical nitrate distribution and drainage profiles on nitrate transport have not been examined in detail.

Exploring the 'nitrate flushing' or 'variable source area' hypothesis in the vertical direction requires examining both the vertical distribution of nitrate mass and vertical variation of hydraulic conductivity simultaneously. When interpreting the enrichment or dilution pattern in the concentration–discharge relationship, most studies with horizontal 'nitrate flushing' hypothesis indicate that it is the new connection with additional nitrate source, that is replenished after a sufficiently long period of disconnection, that brings high nitrate concentration flow downstream (Bowes et al., 2015; Goodridge & Melack, 2012). However, because nitrate concentration depends both on nitrate-outflux and water-outflow from a given location, a more complete explanation may require simultaneously considering both characteristics that determine nitrate-outflux and water-outflow at different levels of local saturation deficit. In this article, we consider how the water-outflow and nitrate-outflux interacts, over a vertical profile, and how they can be influenced by both the vertical distribution of nitrate mass and vertical variation of hydraulic conductivity with depth.

We focus on nitrate and water export from a well-instrumented watershed in southern California. In semi-arid Mediterranean-type watersheds, nitrate and water export is highly episodic and thus lateral expansion and contraction of saturated area may be limited, and vertical flushing processes may be particularly important. In this region, due to the long drought in summer and infrequent but high magnitude and intense rainfall in winter and early spring, most nitrate is exported during wet season during individual storm events (Aguilera & Melack, 2018b; Goodridge & Melack, 2012; Homyak et al., 2014; Parker & Schimel, 2011). In these regions, nitrate mass distribution and hydraulic conductivity decrease with increasing soil

depth. During the long drought in summer, nitrate accumulates in the upper layer because organic material inputs and decomposition rates are higher in near-surface layers (Goodridge & Melack, 2012; Hanan et al., 2016b; Parker & Schimel, 2011). Soil saturated-hydraulic-conductivity typically decays with the soil depth (due to soil structural characteristics such as pore-size distribution) and is commonly represented with an exponential declining function (Ameli, McDonnell, & Bishop, 2016; Beven & Germann, 1982; Beven & Kirkby, 1979). As a result, the distributions of both soil nitrate and soil hydraulic conductivity are biased towards the upper soil layer. When the water table rises, it reaches the upper soil layer with more nitrate and higher hydraulic conductivity, which means it can release more nitrate flux and produce higher volumes of water. During this process, how nitrate concentrations in released water change with declining saturation deficit (or high water tables) is determined by the *rate of change* in soil nitrate flux and the *rate of change* in water flux. This scenario offers a new conceptual model that posits how the vertical distribution of nitrate in soil interacts with the vertical distribution of hydraulic-conductivity, to substantially influence the pattern of concentration–discharge relationships.

In this article, we will explore this conceptual model and how different configurations of the soil hydraulic-conductivity and the soil vertical nitrate distribution influence the concentration–discharge relationships. We address the following questions:

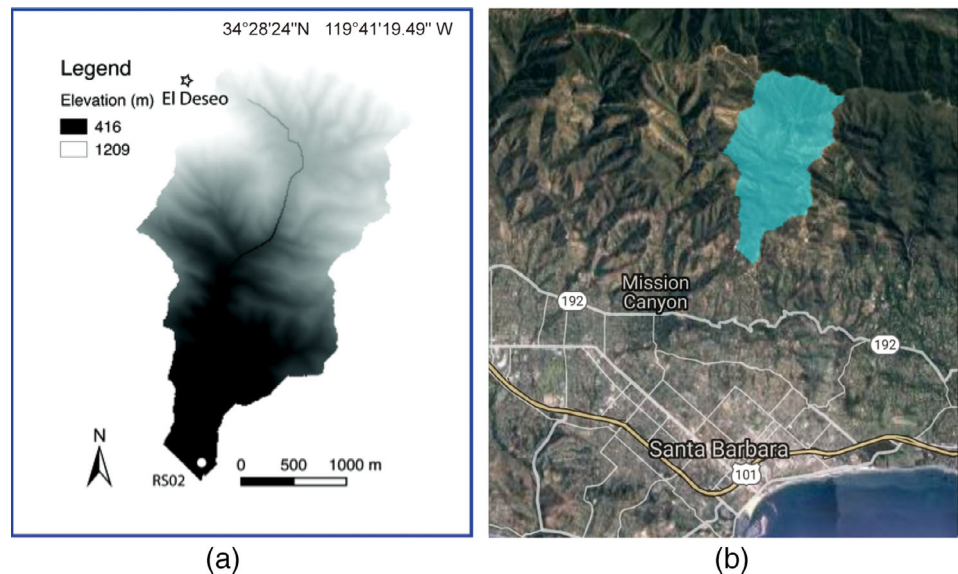
1. How do different configurations of the proposed model (e.g. different combinations of vertical nitrate distribution and hydraulic conductivity distribution) lead to different concentration–discharge patterns at a patch (local one-dimensional) scale in a semi-arid climate? The patch scale represents an average condition where there is no lateral replenishment of water and nitrate flux from upslope areas.
2. Will the different configurations of the proposed model change the concentration–discharge relationship at the watershed scale, where the lateral replenishment between the upland and the downstream patches can also influence nitrate-export?

2 | STUDY SITES AND DATA

2.1 | Study sites

The undeveloped headwater catchment of Rattlesnake Creek, was selected for the study (Figure 1). Rattlesnake Creek watershed (5.8 km² area) is located on the southern facing slopes of the coastal Santa Ynez Mountains and has three dominant shrub species: *Ceanothus megacarpus* (big pod ceanothus), *Adenostoma fasciculatum* (chamise) and *Arctostaphylos* spp. (Manzanita) (Hanan et al., 2016b). The watershed is characterized by steep slopes (slopes >20°) and sandy loams plus rock outcrops. The rainy season lasts from October to April. Large storm events, which last for only a few days, contribute a substantial portion of the annual precipitation. From 2000 to 2009, the mean annual precipitation was 645 mm, with inter-annual variability >360 mm. The streamflow occasionally stops in the long dry summer. The year-round average temperature is 18 °C, with a daily average maximum of 23 °C and a minimum of 13 °C. Atmospheric nitrogen deposition is low:

FIGURE 1 (a) Map for Rattlesnake Creek. 'El Deseo' is the meteorological station used for climate input and 'RS02' provides streamflow data. (Source: LTER data <http://sbc.lternet.edu/data/>). (b) Rattlesnake Creek in Santa Barbara County. (Image Source: 'Rattlesnake.' Google Earth. 34°28'24"N and 119°41'19.49"W. Oct 1, 2018)



0.01 g m⁻² year⁻¹ for ammonium and 0.02 g m⁻² year⁻¹ for nitrate and DON (Goodridge et al., 2018; Santa Barbara Coastal LTER; <http://sbc.lternet.edu//data/dataCollectionsPortal.html>).

2.2 | Data

The climate and discharge data were collected and preprocessed by the Santa Barbara Channel Long Term Ecological Research (SBC LTER) project (Melack, 2012a). Both the stream discharge and the stream chemistry data are from the gauge station 'RS02' (Lon: -119.6922, Lat: 34.4576), which is located at the outlet of Rattlesnake watershed. The original stream hydrologic record was collected as hourly stage values, then converted to discharge using a rating curve with stream channel cross-sections and roughness estimated by the HEC-RAS model. Samples analysed for nutrients were collected weekly during non-storm flows in winter, and bi-weekly during summer. During storms, samples were collected hourly on rising limbs and at 2–4 h intervals on falling limbs. The stream nitrate was measured as 'nitrite + nitrate' in micro-moles per liter (Melack, 2012b), then converted to micro-gram per liter. The precipitation was collected in at 'El Deseo' (Lon: -119.6958, Lat: 34.4917) with a tipping bucket gauge and reported in 5 min interval (J. M. Melack, 2010). Data from 1 October 2004 to 7 October 2005 are used for this study.

Previous studies found that the concentration–discharge relationship in Rattlesnake watershed had an enrichment pattern for storm events (Aguilera & Melack, 2018a; Goodridge & Melack, 2012). In their papers, explanations based on catchment connectivity were provided and suggest that during storm events, more nitrate sources in upland may be connected and more nitrate is flushed downstream, resulting in enrichment. We will provide a model-based analysis that examines how vertical properties described by our conceptual model contribute to the observed concentration–discharge pattern. We configure an eco-hydrologic model, RHESSys (Regional hydro-ecosystem simulation system), to reproduce the enrichment pattern, and discuss the general

implications of the soil vertical nitrate distribution and the hydraulic conductivity distribution on the concentration–discharge relationship.

3 | METHODS

3.1 | Conceptual model

3.1.1 | Saturated hydraulic conductivity and flux of water

We use saturated hydraulic conductivity to describe the rate with which water can move through soil and deeper saprolite layers. Both organic and mineral soil layers as well as underlying saprolite and fractured bedrock are integrated in the model for hydrology and biogeochemical computation. We use the term 'soil' since most of the biogeochemical activity occurs in upper layers that are usually considered as soil, but our conceptual framework does not preclude the flux of water or nitrate through deeper layers. We do not define an explicit soil depth, but rather rely on the exponential decay of saturated conductivity with depth to define an 'effective' soil depth at which low hydraulic conductivity results in negligible lateral flux (Beven & Kirkby, 1979). In order to model lateral flux, we divide the soil into 1000 discrete layers per meter of depth. Soil water outflow rate is calculated as the integration of hydraulic conductivity over these soil layers below the current water table. Because we assume an exponential decay of saturated hydraulic conductivity with depth, a rising water table will lead to an increase of soil water outflow rate and an increase of runoff.

3.1.2 | Soil nitrate distribution in the vertical dimension and nitrate flux

In semi-arid areas, nitrate accumulates near the surface during the dry summer and initial wet-up due to nitrification and the establishment

of micro-scale linkages between microbial sites and substrates needed for nitrification (Goodridge & Melack, 2012; Hanna et al., 2016; Parker & Schimel, 2011). As a result, we assume more nitrate mass in the upper soil layers. Further, in order to understand the influence of vertical nitrate mass distribution and vertical hydraulic conductivity on downstream nitrate concentration pattern, we make some simplifications and assume that the vertical nitrate mass distribution is static overtime. That is to say, although the total mass of nitrate in soil column will change, the nitrate mass distribution in the vertical dimension will not change. This is a necessary simplification and we will discuss it in the following sections.

In our conceptual model, nitrate within the water table can be transported by saturated subsurface flow; in unsaturated soil, there is no lateral transport of nitrate. Nitrate outflux from a patch is proportional to the soil nitrate mass within the soil layer where saturated lateral flux occurs. The distribution of soil nitrate mass in a soil layer follows an exponential decay function (Tague & Band, 2004), with more soil nitrate mass at the surface layer and less at depth. The total soil nitrate flux is calculated as the integration of the nitrate-outflux for each soil layer below the soil water table.

$$N_{\text{output_layer}}(\text{Sat}_{df}) = Qdf \times N_{\text{all}} \times \exp(-N_{\text{decay}} \times \text{Sat}_{df}) \times N_{\text{decay}} \quad (1a)$$

$$\begin{aligned} \text{Total Nitrate Outflux}(\text{Sat}_{df}) &= \int_{\text{Max_Sat}_{df}}^{\text{Sat}_{df}} N_{\text{output_layer}}(\text{Sat}_{df}) = Qdf \\ &\times N_{\text{all}} \times (\exp(-N_{\text{decay}} \times \text{Sat}_{df}) - \exp(-N_{\text{decay}} \times \text{max_sat}_{df})) \quad (1b) \end{aligned}$$

where Sat_{df} is the soil saturation deficit, max_sat_{df} is the maximum soil saturation deficit and $N_{\text{output_layer}}(\text{Sat}_{df})$ is the nitrate mass output from the patch in the soil layer at the current water table. Qdf is the lateral transport of water from the patch at soil saturation deficit Sat_{df} . N_{all} is the leachable amount of soil nitrate in that patch. At any point in time N_{all} reflects the time varying impact of multiple N-cycling processes.

$$N_{\text{all}}(t) = N_{\text{all}}(t-1) - N_{\text{uptake}}(t) + N_{\text{microbial_net}}(t) + N_{\text{input}}(t)$$

N_{uptake} reflects the plant uptake of nitrate by roots; $N_{\text{microbial_net}}$ is the net nitrate released to the soil by microbial processes, predominately decomposition of decaying plant organic matter and subsequent nitrification and denitrification processes; $N_{\text{microbial_net}}$ can be negative when microbial immobilization is high, N_{input} is nitrate inputs through atmospheric deposition and other surface sources such as fertilizers. N_{all} here is the mobile nitrate or nitrate in excess of soil adsorption. We note that the focus of this article is the flushing of nitrate from the soil column during storm events rather than the seasonal soil microbial and vegetation processes that give rise to N_{all} . Nonetheless because seasonal temporally synchronicity or asynchronicity between these processes and flushing can be important we include them in our conceptual framework and provide a brief description of how they are modeled in RHESSys below.

In our conceptual model, we assume that N_{all} is distributed through the upper soil profile with an exponential distribution characterized by N_{decay} (the vertical decay rate of the nitrate with depth). A high N_{decay} corresponds to more unevenly distributed nitrate in soil, with most of the nitrate gathering in top layers, and a lower N_{decay} corresponds to a more evenly distributed situation. The integration of $N_{\text{output_layer}}(\text{sat}_{df})$ from max_sat_{df} to sat_{df} , which can be interpreted as the total nitrate flux below water table, also follows the exponential distribution.

Soil water outflow is calculated following the 'continuous exponential' transmissivity model (Beven & Kirkby, 1979), where both the subsurface conductivity and transmissivity decay exponentially with the soil saturation deficit:

$$K(\text{sat}_{df}) = K\text{sat}_0 \times \exp(-\text{sat}_{df} \times K_{\text{decay}}) \quad (2a)$$

$$\text{Soil Water Outflow} = T(\text{sat}_{df}) = \int_{\text{max_sat}_{df}}^{\text{sat}_{df}} K(\text{sat}_{df}) \quad (2b)$$

where $K(\text{sat}_{df})$ is the hydraulic conductivity when the soil saturation deficit equals sat_{df} , max_sat_{df} is the maximum of saturation deficit, $K\text{sat}_0$ is the saturated hydraulic conductivity at surface soil, $T(\text{sat}_{df})$ is the transmissivity when the soil saturation deficit equals to sat_{df} , and K_{decay} is the coefficient controlling the decreasing rate of transmissivity against the soil saturation deficit.

Nitrate concentration in output flux is then calculated as

$$\text{Concentration} = \frac{\text{Total Nitrate Outflux}}{\text{Soil Water Outflow}} \quad (3)$$

Nitrate concentration is dynamic in model simulations and is determined by both Total Nitrate Outflux and Soil Water Outflow. Since the vertical distribution of nitrate mass and hydraulic conductivity control Total Nitrate Flux and Soil Water Outflow, these two parameters (vertical distribution of nitrate mass and hydraulic conductivity) also affect the nitrate concentration in the released water.

3.1.3 | Vertical profile controls on the concentration–discharge relationship: A simple demonstration

Patch scale

First, we present a hypothetical case for which available soil nitrate mass increases faster than the hydraulic conductivity as the water table rises (or saturation deficit decreases) (Figure 2). In other words, the rate of change for soil nitrate mass is greater than the rate of change for the hydraulic conductivity along the vertical direction. These soil nitrate and soil hydrological parameter settings result in an enrichment pattern in the concentration–discharge relationship (Figure 2F).

Following this same approach, we created a scenario to explain a dilution pattern (Figure 3). The key difference between the two cases

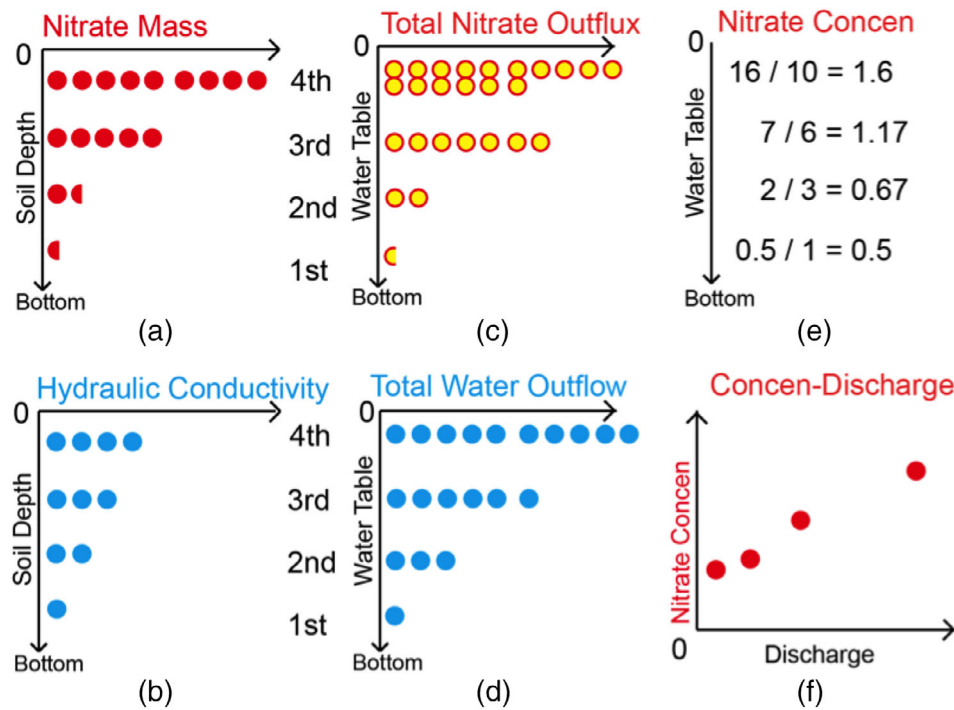


FIGURE 2 Cases with soil nitrate distributed unevenly with soil depth (a), and with hydraulic conductivity unevenly distributed with depth (b). These scenarios result in an enrichment concentration–discharge pattern (f) as the water table rises from the first to fourth soil layer (nearer to the surface). Points in subplots a, b, c, d and f represent: one unit of nitrate (a), one unit of hydraulic conductivity (b), one unit of total nitrate outflux (c), one unit of water outflow (d) and one unit of concentration (f). Subplots 2a and 2d are derived from subplots 2a and 2b by integrating water and nitrate flux from the corresponding soil layers. For example, the total nitrate outflux when water table reaches the third soil level is the summation of nitrate fluxes for the lower three layers, proportional to the nitrate mass distribution in these three layers, that is, $0.5 + 1.5 + 5 = 7$. Following the same method, the total nitrate out flux when water table reaches the surface is $0.5 + 1.5 + 5 + 9 = 16$ unit flux. The total water outflow when water table reaches the third level is $1 + 2 + 3 = 6$ unit water flow. When the water table reaches the surface, water flux is $1 + 2 + 3 + 4 = 10$ unit water flow. Subplot 2e shows the nitrate concentration at each water table level computed using the total nitrate outfluxes divided by total water outflow (Equations 1a and 1b)

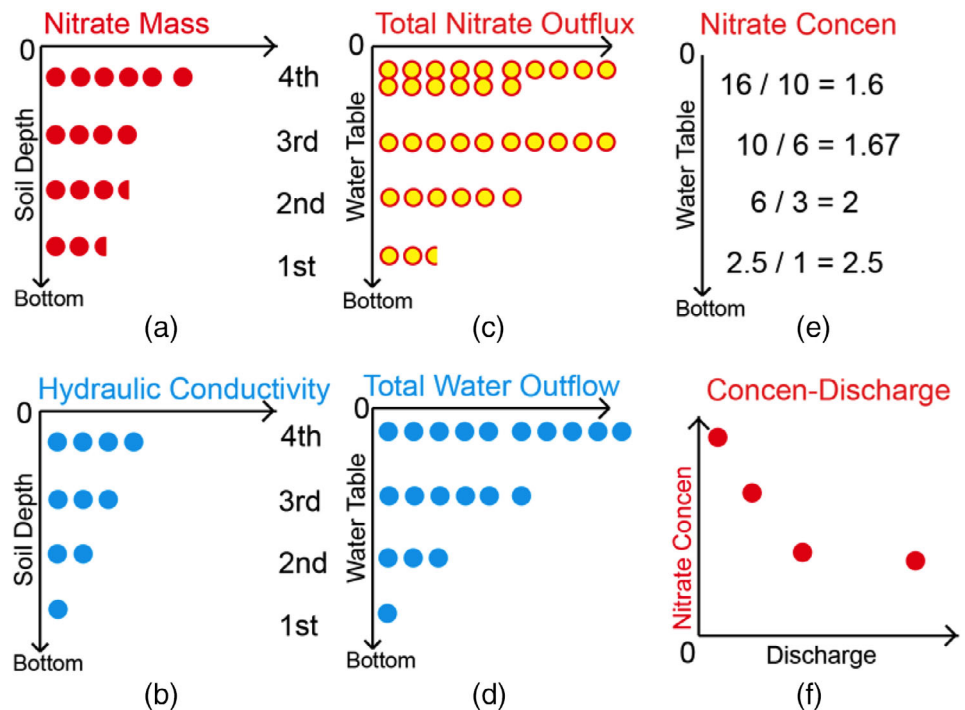


FIGURE 3 A scenario with nitrate is less unevenly distributed compared with Figure 2, resulting a dilution pattern. Points in subplots a, b, c, d and f represent one unit of nitrate (a), one unit of hydraulic conductivity (b), one unit of nitrate flux (c), one unit of water out flow (d) and one unit of concentration (f). Subplots 3c and 3d are derived from 3a and 3b by integrating water and nitrate flux from the corresponding soil layers

is indicated by the nitrate mass distributions in Figures 2A and 3A. In Figure 3, nitrate is more evenly distributed over vertical soil profile (Figure 3A) (the rate of change for nitrate mass is less than the rate of change for hydraulic conductivity), although there is still more nitrate in upper soil layers. Water flux and the distribution of hydraulic conductivity with depth in Figure 3 are the same as in Figure 2. However, the nitrate concentration in this scenario has a dilution pattern with a rising water table. Thus, a small change in the vertical distribution of nitrate mass can result in an abrupt change in concentration–discharge relationship (Figure 3F vs Figure 2F).

Watershed scale

At the watershed scale, sources of nitrate include lateral inputs from upslope patches. The replenishment of soil nitrate in receiving patches during the storm events results in more complicated scenarios.

At the watershed scale, lateral flow combines with vertical nitrate distribution and hydraulic conductivity to regulate the concentration–discharge relationship (Figure 4). Without lateral nitrate replenishment, the concentration–discharge relationship would show a dilution pattern. With additional nitrate replenishment from upslope area, the concentration–discharge relationship would shift from dilution to enrichment. If this patch is a riparian patch near stream, then the resulting nitrate export will have direct influence on the concentration–discharge relationship of the stream. In this case, the concentration–discharge relationships reflect both vertical and lateral ‘flushing’ phenomena.

3.2 | RHESSys model description

The description above provides an illustration of how the vertical soil drainage properties and vertical nitrate distribution can interact to influence concentration–discharge relationships. To assess how these factors influence nitrate concentration–discharge relationships for a more realistic situation where water and nitrate evolve dynamically, we configured vertical nitrate distribution and hydraulic conductivity in the Regional Hydro-Ecologic Simulation system (RHESSys) and tested the sensitivity of the concentration–discharge relationship to these configurations. RHESSys is a physical process-based, distributed hydrological model, which has been widely implemented in a variety of bioclimatic regions, including in semi-arid regions (López-Moreno et al., 2014; Shields & Tague, 2012; Tague, Seaby, & Hope, 2009). RHESSys explicitly models the catchment connectivity by calculating the volume of water exported from upland to downstream via lateral movement through adjacent patches (Tague & Band, 2004). The soil profile is represented in two layers: an unsaturated layer and a saturated layer. The unsaturated layer contains a root zone layer. The water held in saturated and unsaturated layers is updated following infiltration. The vertical infiltration from surface detention to the unsaturated layer follows the Philip's infiltration equation (Philip, 1957). Time to ponding is approximated using the Green and Ampt method (Green & Ampt, 1911). Drainage from the unsaturated layer to the saturated layer is controlled by the field capacity of the unsaturated layer and by the vertical hydraulic conductivity at the boundary between unsaturated and

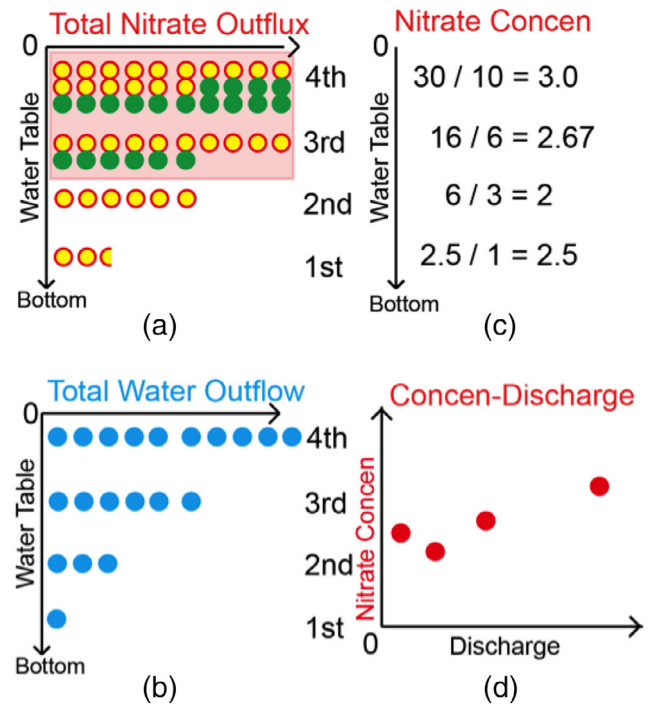


FIGURE 4 At watershed scale, lateral nitrate replenishment will change the concentration–discharge relationship from dilution in Figure 3f to enrichment in Figure 4d. The green points are results of lateral nitrate replenishments from upland. All the other labels follow the same definitions as Figures 2 and 3. Without the lateral nitrate replenishment, the nitrate outflux is the same as that in Figure 3 and the concentration–discharges relationship would show a dilution pattern. However, assuming that when the water table rises to the third level, lateral water movements bring nitrate replenishments from upland to this patch, increase the total nitrate outflux and changes the nitrate concentration. The resulting nitrate concentration with the rising water table is now 2.5, 2, 2.67 and 3.0 units, and is thus an enrichment rather than dilution pattern in Figure 3E,F

saturated layer (Tague & Band, 2004). Lateral flow is calculated only in the saturated layer, not in the unsaturated layer. The ‘continuous exponential’ transmissivity model (Beven & Kirkby, 1979) for subsurface flow sub-model is used to calculate the subsurface lateral flow, where both the subsurface conductivity and transmissivity decay exponentially with the soil saturation deficit (Equation 2).

A flow network partitions this subsurface from a given patch to downslope neighbors based on topographic gradients. During preprocessing, the flow network is generated by a GIS-based routine, assuming that the hydraulic gradient follows the surface topography. In the routing model, more than one downslope patch can receive lateral flow from a given upslope patch. We acknowledge that bedrock topography plays an important role for the subsurface flow on hillslope (Freer et al., 2002; Graham, Woods, & McDonnell, 2010). Because of the steep slope/shallow soil layer in the study area and lack of bedrock measurement data, surface topography is used to calculate the hydraulic gradient.

Evaporation and transpiration including evaporation of rain intercepted by each canopy layer, and transpiration of vascular layers, are calculated using Penman Monteith approach (Monteith, 1965) at a daily

timestep. Soil evaporation is calculated based on energy and atmospheric drivers as well as a maximum exfiltration rate. The maximum exfiltration rate is determined by soil parameters and soil moisture. Potential capillary rise is constrained by soil parameters and the water table.

RHESSys calculates biogeochemical cycling similar to those in BIOME-BGC (Thornton, 1998) and other Dynamic Global Vegetation Model (DGVM) models such as CLM (Oleson et al., 2004). Photosynthesis and respiration are modeled at a daily time step, with adjustments to account subdaily radiation patterns and their seasonal variation (Tague & Band, 2004). Photosynthesis (and transpiration) is computed separately for sunlit and shaded leaves. Net carbon assimilation (photosynthesis minus respiration) is allocated to plant carbon stores to simulate growth. In RHESSys, carbon and nitrogen stores are partitioned into leaves, roots, live and dead stems, and coarse roots, each with distinctive C:N ratios and respiration rates. Vegetation nitrogen stores and carbon stores are linked following the stoichiometric relationships. Plant component turnover rates are based on species-specific parameters. Decomposition is based on partitioning newly fallen organic matter into litter and soil pools with distinctive C:N ratios with pool-specific decay rates that are modified by temperature and moisture availability. Nitrification and denitrification are modeled following the CENTURY_{NGAS} approach (Parton et al., 1996) that account for soil moisture, carbon substrate availability, soil temperature and pH controls on these processes. RHESSys also includes an estimation of N adsorption as a function of soil type, following Kothawala & Moore (2009). The parameters for biogeochemical reaction, such as decomposition and decay rates, follow the set up from a previous study in the same area (Hanan et al., 2016b; Shields & Tague, 2012). Although RHESSys can explicitly model nitrification and denitrification, the nitrate-related biogeochemical processes are not likely to be the main reason for the changes in the concentration–discharge pattern during storm events

in these steep coastal mountain watersheds (Goodridge & Melack, 2012; Meixner et al., 2007). Hence, on a time scale of days, hydrological transport was emphasized in our analyses.

In the soil column, the vertical distribution of nitrate mass is assumed to follow an exponential distribution, with more soil nitrate mass at the surface layer and less at depth. The nitrate-outflux at each soil layer is proportional to the soil nitrate mass at that layer. The total soil nitrate flux is calculated as the integration of the nitrate-outflux for each soil layer below the soil water table (Equation 1). As the result, the total soil nitrate flux also follows an exponential distribution.

3.2.1 | Groundwater


In RHESSys, the groundwater pool is simulated to approximate the store and release of groundwater. However, in this steep headwater catchment, the complex, fractured bedrock and lack of groundwater measurements make it difficult to analyze the contribution of groundwater to the downstream nitrate concentration–discharge patterns. Furthermore, while deep groundwater may substantially contribute baseflow, shallow subsurface and surface flowpaths likely dominated stormflow responses. For simplicity, we do not include deep groundwater outputs in our analysis of this study that focuses on storm flow responses.

The model set-up is illustrated in Table 1.

3.2.2 | Key assumptions

Our conceptual model and its implementation within RHESSys include several key assumptions. We emphasize the importance of soil vertical nitrate distribution and its interactions with lateral subsurface

TABLE 1 Model set-up for single patch and watershed scale scenarios

		
Scenarios	Single patch scale	Watershed scale
Initial topography	Spatial averaged slope/aspect	DEM
Vertical hydrologic process	Infiltration, unsaturated and saturated zone drainage (exponential decay of K with depth)	
In-situ N-cycling	Vegetation uptake, microbial litter and soil organic matter decomposition, nitrification/denitrification, N-leaching with saturation zone drainage	
Lateral hydrologic process	Saturated subsurface and any surface water (infiltration or saturation excess) routed between patches and to stream based on topographic gradients	

Note: The major difference is in the lateral hydrologic process in patch scale scenario, the whole watershed is treated as a single patch and no lateral replenishment is considered. In watershed scale scenario, lateral replenishment is included. For vertical hydrologic/transport process and in-situ N-cycling, both scenarios share the same processes. Further description of each process can be found in Tague and Band (2004).

flow. To do so we assume that (1) lateral nitrate export occurs only in the saturated layer; (2) soil vertical nitrate mass distribution is proportional to the lateral nitrate out flux distribution at each soil layer; (3) although the total nitrate mass in soil column may change, the soil vertical nitrate mass distribution is static.

The first and second assumptions can be written as

$$\text{NO3}_{\text{flux}}(d) = \frac{\partial \text{NO3}(d)}{\partial t} = \text{Sat}_d \times \text{NO3}(d) \quad (4)$$

where $\text{NO3}_{\text{flux}}(d)$ is the lateral nitrate out flux from soil layer at depth d , $\text{NO3}(d)$ is the nitrate mass from soil layer at the depth d , Sat_d is the dummy variable representing whether this layer is saturated or not. If soil layer at depth d is not saturated, then Sat_d is 0. Otherwise, it is a non-zero constant. In this study, we focus only on lateral nitrate export in saturated layer to demonstrate how interactions between vertical nitrate distributions and hydraulic conductivity can shift between enrichment and dilution states. Using this assumption, the distribution of nitrate flux at each soil layer is deduced from the distribution of nitrate mass, and the total nitrate flux is calculated by the integration of nitrate flux from each soil layer beneath the current water table. This article makes several key assumptions about the distribution of nitrate in the subsurface and the dominant flowpaths that transport that nitrate. While sensitivity of N-decay explores the implications of how evenly distributed the nitrate is in the subsurface, we always assume an exponential decay. There may be situations where nitrate increases with depth (e.g. locations where septic leakages occurs or where deep groundwater storage and drainage of nitrate are a significant contribution to nitrate export). In this study, we focus on shallow subsurface flowpaths that provide water for storm and recession flows. Additional analysis of deeper groundwater contributions can be explored in the future work.

Third, we assume that the shape of nitrate mass distribution with depth does not vary through time. In other words, even though the total nitrate mass in soil column changes, how it is distributed with depth does not change. This assumption follows the nitrate-flushing hypothesis (Creed et al., 1996; Tague & Band, 2004). We acknowledge that nitrate distributions are likely to change as environmental conditions change. For example, after long drought, nitrate may accumulate near to the top layer, resulting in a more uneven N distribution (Goodridge & Melack, 2012). After sequences of large rainfall events, the nitrate from top layer may infiltrate into deeper soil layers. We note, however, that field investigations also suggests that the infiltrating water may move through unsaturated layers via macropores, without significant contact with the soil matrix (McDonnell, 1990; Peters, Buttle, Taylor, & Lazerte, 1995) and thus this redistribution of nitrate with infiltration may not occur. Further, in this study, we focus on longer term controls on vertical nitrogen distribution related to soil structure that do not change with time to show their importance in determining patterns of nitrate export. Total nitrate changes, however, are modeled to maintain a nitrogen balance, including nitrate losses due to flushing, plant uptake and nitrate generating through organic matter decomposition and nitrogen deposition.

3.3 | Simulations and analysis

3.3.1 | Initial calibration

During the initial hydrologic calibration, 3000 Monte Carlo daily streamflow simulations were implemented by varying 3 parameters (K_{decay} and K_{sat0} as well soil depth), with the top 150 parameter sets resulting in a Nash-Sutcliffe Efficiency (Nash & Sutcliffe, 1970) range from 0.63 to ~0.79. After the initial calibration, a constant decay rate for soil hydraulic conductivity (K_{decay}) and a constant soil depth were selected by calculating the median value within the top 150 parameter sets. We then use these values to investigate the influence of different combinations of N_{decay} and K_{sat0} pairs on the concentration–discharge patterns.

3.3.2 | Simulation for sensitivity analysis

By varying the vertical soil nitrate distribution parameter N_{decay} , we assess the impact of nitrate vertical distribution on nitrate concentration–discharge pattern downstream. A range of saturated soil hydraulic conductivities (K_{sat0}) was used to vary the relationship between water flux and nitrate flux and evaluate the effects on nitrate concentration. Previous applications of RHESSys in this watershed, have evaluated model hydrologic performance (Shields & Tague, 2012) and plot scale nitrogen cycling (Hanan et al., 2016b). The range of values of key parameters (N_{decay} , K_{sat0}) overlaps with the settings in the previous modeling studies (Hanan et al., 2016b) or derived from previous studies (Demenico & Schwartz, 1990). Values for K_{decay} are within ranges estimated in previous hydrologic studies in this region (Shields & Tague, 2012). All the other parameters use standard values from RHESSys parameter libraries for chaparral ecosystems.

All the simulations were run on both the patch scale (a) and watershed scale (b).

(a). Simulations for combinations of N_{decay} and K_{sat0} on single patch scale.

Simulations were driven using daily observed meteorological data from 1 October 2004 to 7 October 2005. For the patch scale simulations, the Rattlesnake Creek watershed is treated as a single patch, and assigned a set of spatially averaged soil and vegetation parameters. The drainage area is around 5.8 km². In this lumped case, there is no lateral subsurface flow within the watershed. Three hundred and thirty-six different pairs of N_{decay} and K_{sat0} were tested, with 21 values between [2, 6] for N_{decay} and 16 values between [1, 1,200] (m/day) for K_{sat0} (Table 2). The lowest value of N_{decay} corresponds to the more even nitrate distribution in the vertical dimension. The highest value of N_{decay} refers to the vertical nitrate distribution where nitrate is most preferentially distributed near to the surface.

(b). Simulations at the watershed scale.

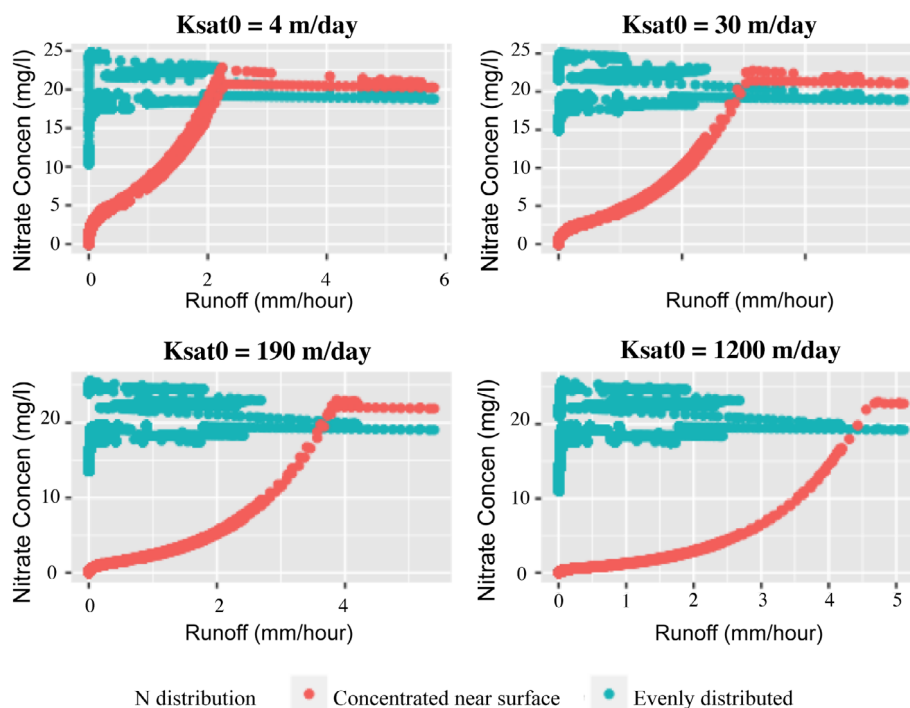
RHESSys model was set up with ~2000 patches using a DEM with 30-m resolution from SBC LTER database (Melack, 2010). Lateral

TABLE 2 Parameter ranges for model simulations in single patch scale and watershed scale*

	N_decay rate for patch scale (unitless)	N_decay rate for watershed scale (unitless)	Hydraulic_Conductivity (m/day)
Min	2 (more evenly distributed)	0.1 (more evenly distributed)	1
Max	6 (more in upper layer)	10 (more in upper layer)	1200

*From *Physical and Chemical Hydrogeology* (Demenico & Schwartz, 1990), the hydraulic conductivity ranges from 8×10^{-13} m/s (unweathered marine clay) to 3×10^{-2} m/s (gravel). Considering the sandy soil in the study area, the hydraulic conductivity at soil surface was set from 1×10^{-5} m/s (silt) to 3×10^{-2} m/s (gravel), which is roughly 1 to 1200 m/day.

FIGURE 5 Concentration–discharge plot for a single patch for increasing values K_s at 0 and 2 contrasting vertical distributions of nitrate. The red points show results when nitrate distribution is concentrated near the surface ($N_{\text{decay}} = 6$). The blue points are the nitrate concentrations for distributions with nitrate more evenly distributed ($N_{\text{decay}} = 2$)



subsurface replenishment is included in this scenario. Based on initial simulation results, the parameter sensitivity of N_{decay} on stream nitrate concentration changes with spatial scale (patch vs watershed). As a result, a wider range of N_{decay} than that from the patch scale simulations was used in the watershed-scale simulation. Together with the hydraulic conductivity, 336 parameter sets were tested (Table 2), with observed input data from 1 October 2004 to 7 October 2005. Parameters were assumed to be spatially homogeneous throughout the watershed.

4 | RESULTS

4.1 | RHESSys modeling on single patch scale

By varying N_{decay} and K_{sat0} , 336 scenarios were simulated using the RHESSys model. Results for several examples with $K_{\text{sat0}} = 4, 30, 190$ and 1200 m/day and $N_{\text{decay}} = 2$ (evenly distributed) and 6 (concentrated near surface layers) are illustrated in Figure 5.

When $N_{\text{decay}} = 2$ (blue circles, relatively evenly distributed nitrate), the nitrate concentration–discharge patterns have a flat or

slight dilution pattern across a wide range of K_{sat0} values. In contrast, when nitrate is preferentially located near to the surface ($N_{\text{decay}} = 6$ red circle), the nitrate concentration tends to have enrichment patterns. This is consistent with our simple illustrative model where more evenly distributed soil nitrate tends to produce a dilution pattern (Figure 2), and scenarios where nitrate is concentrated nearer to the surface produces an enrichment pattern. The higher N_{decay} (red circle) scenario leading to enrichment is more sensitive to changing K_{sat0} than the dilution pattern associated with a lower N_{decay} (blue circle). When N_{decay} is high, for lower values of K_{sat0} , enrichment tends to plateau at higher runoff. For higher K_{sat0} enrichment occurs even for high runoff. When N_{decay} is high, concentrations tend to be lower for lower K_{sat0} across most runoff values.

To show how concentration–discharge patterns vary across a wider range of N_{decay} and K_{sat0} values, we calculated the slope of concentration–discharge plots for storm flow to quantify patterns in the storm flow concentration–discharge relationship. For each concentration–discharge plot (Figure 5), we define the storm flow as any runoff larger than 97.5% of the runoff in the water year 2005

(1.3 mm/h). Then, for the points with discharge larger than 1.3 mm/h, we applied ordinary linear regression,

$$\text{Concentration} = a + \text{slope} \times \text{discharge} \quad (5)$$

and obtained the slope of the discharge as the average rate of change in concentration–discharge during storm events. For each N_{decay} and K_{sat0} pair, a corresponding ‘slope’ value was calculated. As a result, the 336 ‘slope’ values (Figure 6) describe the overall trend of the storm flow concentration–discharge relationship (Figure 5) for each of the 336 scenarios. Among them, positive ‘slope’ shows the enrichment pattern; negative ‘slope’ shows the dilution pattern; a ‘slope’ of 0 represents a stable pattern.

Both N_{decay} and hydraulic conductivity K_{sat0} control average trend of the concentration discharge relationship during storm flow (Figure 6). Higher N_{decay} scenarios (yellow and red) generally result in a steeper positive slope (with value larger than 4), corresponding to a stronger enrichment pattern. Lower N_{decay} cases (blue and black) result in a flat or negative slope (with value less than 0), representing a stable or dilution pattern. Hydraulic conductivity K_{sat0} also affects the average slope. With the increase of hydraulic conductivity, the average slope of enrichment curve in high N_{decay} cases (red) increases, and the average slope in low N_{decay} cases (blue and black) remains low. However, there is a threshold conductivity value (~500 m/d) at which the slope of enrichment curve of high N_{decay} case (red) reaches its maximum and then declines. This decline occurs because soil with higher hydraulic conductivity drains water faster than soil with lower hydraulic conductivity. With higher soil hydraulic conductivity, it is more difficult for the water table, and thus subsurface flow, to reach top layer and export the greater nitrate mass from the surface soil layer. Reduced access to upper soil layers means it is less likely that a stronger enrichment pattern will occur. As a result,

when K_{sat0} exceeds the conductivity threshold, the slope of enrichment curve begins to decline slightly.

4.2 | Simulations with RHESSys model in watershed scale

We first examine results for several illustrative scenarios at the watershed scale (Figure 7a–c), and then present summary metrics for simulations across all values of N_{decay} and K_{sat0} (Figure 8a,b). Since these simulations are at the watershed scale, subsurface lateral flow moves from upland areas through the riparian zone to the stream through a series of adjacent, connected patches. The resulting pattern and magnitude of responses to precipitation and N_{decay} and K_{sat0} parameters differ from that in patch scale (Figure 5). To better show the patterns of concentration–discharge relationships, we plot the x-axis in log-plot and use the linear regression line to represent the general trend of concentration–discharge relationship. We also include concentration–discharge relationships derived from observed measurements for comparison.

In Figure 7a, the modeled concentration–discharge plot (black circles) has a two-stage pattern: an enrichment for runoff <0.07 mm/h, then a dilution for runoff >0.07 mm/h, with the ‘transition point’ at peak concentration with runoff = 0.07 mm/h (Figure 7a). The observed concentration–discharge also has a two-stage pattern; however, its transition period is at runoff = 0.2 mm/h, which is greater than the simulated transition runoff. In order to evaluate the impact of parameters on the concentration–discharge relationship, two linear regression lines are plotted to represent the average slope for the enrichment stage and dilution stage. The sensitivity of these slopes to parameter values are presented in Figure 8a,b and discussed in more detail below. To help explain modeled watershed scale patterns, we

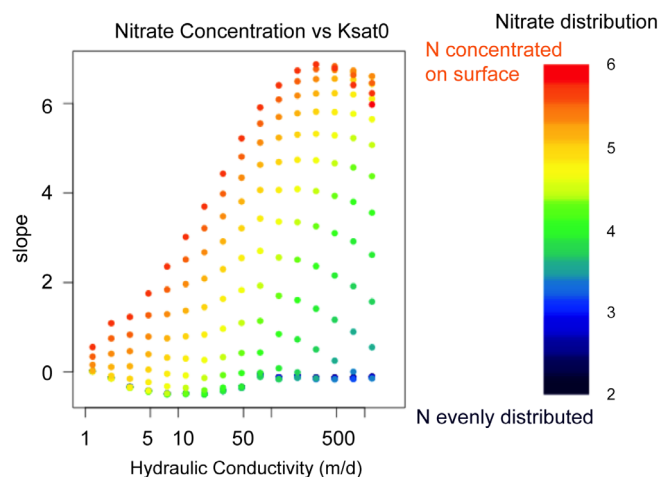


FIGURE 6 Average slope for nitrate concentration plots for storm runoff in the 336 simulations. Each point represents the average slope of the concentration–discharge relationship. Red points represent scenarios with a more uneven distribution of nitrate (e.g., nitrate more concentrated at the surface). Black or blue points represent more evenly distributed scenarios. The x-axis is the hydraulic conductivity. y-axis is the average slope. A greater positive average slope corresponds to stronger enrichment, while a more negative average slope corresponds to stronger dilution

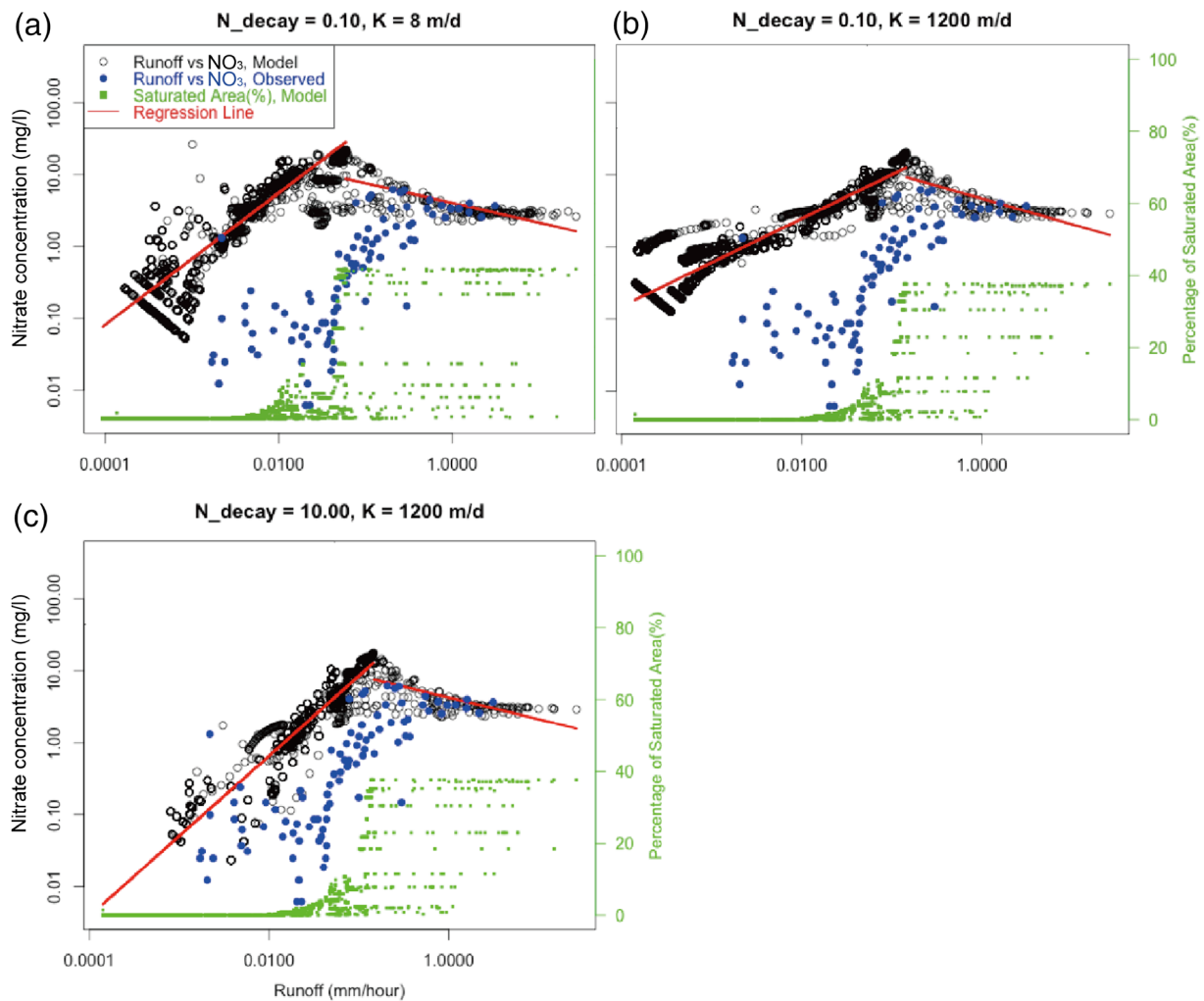


FIGURE 7 Runoff versus concentration. (a) $N_{decay} = 0.1$, Hydro_Conductivity (K_{sat0}) = 8 (m/day). (b) $N_{decay} = 0.1$, Hydro_Conductivity (K_{sat0}) = 1,200 (m/day). (c) $N_{decay} = 10$, Hydro_Conductivity (K_{sat0}) = 1,200 m/day. Blue points are the observed concentration–discharge points, black points are the concentration–discharge results from model (in daily timestep), the green dots are the percentage of saturated area from model, and the red line is the regression line for the modeled concentration–discharge relationship. The transition point from ‘rising’ to ‘plateau’ stage in the percent-saturated area (green dots) corresponds to a transition point where the concentration–discharge shifts from enrichment to dilution (black points)

use ‘percent saturated area’ (green dots), which defines the percent of the watershed where the modeled water table is at the surface. Percent saturated area has a three-stage pattern (dry, rising and plateau) with transitions when runoff reaches 0.005 mm/h and again at 0.07 mm/h. During the ‘dry stage’, between runoff 0.0001 and 0.005 mm/h, the water table is below the surface for the entire watershed (0% saturated area). Then, during the initial wetting up following precipitation, patches near stream become saturated and the saturated area expands with more precipitation. As runoff increases from 0.005 to 0.07 mm/h, the percent saturated area increases from 0 to 41% (rising stage). After the rising stage, it goes into the ‘plateau’ stage. At this stage, the percent saturated area remains at 41% but the runoff increases from 0.07 mm/h to over 7 mm/h, indicating that fast flowpath or overland flow is contributing to the increase in runoff. The transition point (0.07 mm/h) in percent saturated area from ‘rising’ to ‘plateau’ stage corresponds the transition point (0.07 mm/h)

in the concentration–discharge relationship pattern that shows a shift from enrichment to dilution. This is not by chance, and we will explain it in a few paragraphs.

In Figure 7b, while the overall pattern is similar to that for Figure 7a, the transition point, between enrichment and dilution, occurs at higher runoff values, from 0.07 to 0.2 mm/h. In other words, the increase of K_{sat0} from 8 to 1200 m/day has moved the transition point rightwards. The lowest nitrate concentration also increases from 0.04 to 0.1 mg/L. As a result, the slope of regression line of the ‘enrichment stage’ is flatter in Figure 7b than in Figure 7a. Increases in saturated area occur at higher runoff values, such that initiation of the ‘rising’ stage in percent saturated area shifts from 0.005 to 0.01 mm/h. The starting runoff value for the ‘plateau’ stage shifts from 0.07 to 0.2 mm/h. Again, the transition point of ‘percent saturated area’ still corresponds to the transition point of concentration–discharge relationship.

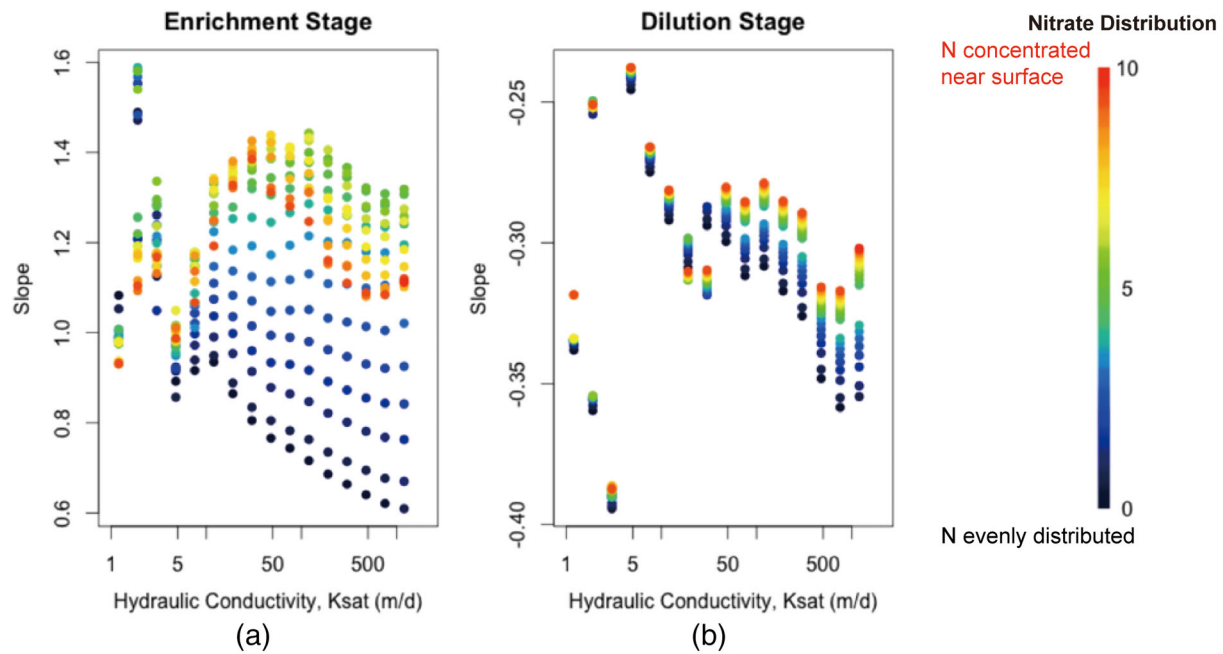


FIGURE 8 Slope of regression lines for concentration–discharge plot during the ‘enrichment’ stage (a) and the ‘dilution’ stage (b). x-axis is the hydraulic conductivity and y-axis is the slope of the regression line. Red and yellow points represent scenarios with higher N_{decay} . Blue and black points represent scenarios with lower N_{decay} . Higher absolute value in slopes represents stronger enrichment or dilution patterns. Figure 8b shows that the sensitivity of slopes to vertical nitrate distribution is lower in dilution stage than in enrichment stage

In Figure 7a,b, the overlap of the transition points indicates that there may be a shared mechanism for the transition to the ‘plateau’ in percentage saturated area plot and to the ‘dilution’ in the concentration–discharge plot. As mentioned above, the ‘plateau’ stage for percent saturated area reflects an increase in the importance of fast flow paths or overland flow that result in an increase in runoff without an expansion in saturated area. These fast flow paths may also contribute to dilution since water traveling through these pathways is unlikely to access additional nitrate once initial wash-off of surface nitrate from the deposition has been depleted earlier in the storm. As a result, although the fast flow paths can drain a substantial amount of water into streams, the lateral nitrate replenishment is limited. Thus, as contributions from these flow paths increase, nitrate concentrations decrease. (Figure 7a,b) With the $K_{\text{sat}0}$ increases from 8 to 1200 m/day, the watershed drainage capacity increases, postpones the generation of overland flow, and shifts the dilution transition point to larger discharge rate.

In Figure 7c, the increase of N_{decay} from 0.1 to 10 contributes to several differences between Figures 7a–c: the most substantial change is the lower nitrate concentration for low flow condition in the ‘enrichment’ stage (left of the transition point) in Figure 7c, which resulting in a steep slope for the concentration–discharge plot in the ‘enrichment’ stage. This is because with higher N_{decay} (Figure 7c), more nitrates will be concentrated on the surface, and fewer nitrates export will be exported during wetting up period, compared with low N_{decay} scenario (Figure 7a).

Figure 7c shows the concentration–discharge curve that is quite similar to the observed one. There is however a clear overestimation

of concentrations in the enrichment stage. This discrepancy may be related to other parameters/variables beyond the two parameters that are the focus of this study. RHESSys is likely overestimating nitrate production, which may be related to vegetation uptake, microbial decomposition, or nitrification/processes as well as potentially losses of nitrate to deeper groundwater flowpaths. There are several key simplifications in the implementation of RHESSys at this site that may contribute to the overestimate of N production. N-uptake by plants varies seasonally and comprises a substantial component of the N budget in these chaparral systems and can vary with species and biomass (Goodridge et al., 2018; Homyak et al., 2014; Rundel, 1982). The current implementation uses parameters that reflect the average of chaparral species. RHESSys representation of the timing and rate of litter fall may be another factor to explain the discrepancy. Other studies have shown that variation in vegetation dynamics can substantially alter the N-availability in the soil. Miller, Schimel, Meixner, Sickman, and Melack (2005), for example, show that litter additions substantially reduced N-mineralization and the leaching of inorganic N from chaparral soils (Miller et al., 2005). Earlier studies also show chaparral species differences in the timing of litter decomposition and the release of N (Schlesinger, 1985). Currently RHESSys estimates litter fall as a percentage of aboveground biomass and does not vary the timing of litter fall with climate. The current approach used to estimate litter fall along with the assumption of a single species and its associated N-uptake dynamics are likely candidates that may contribute to bias in estimates of available N for leaching at different times through the season. Further work to refine the parameters and inputs (such as vegetation cover maps) and more detailed groundwater

modeling could be used to improve estimates. Again, we note that the goal here is not to provide the 'best estimate' of the concentration–discharge but to explore how interactions between the vertical profile of nitrate and hydraulic parameters can influence concentration–discharge patterns.

To reveal the patterns in the concentration–discharge relationship in 'enrichment' and 'dilution' stages, regression lines are constructed and the slope of regression lines are calculated to compare the sensitivity of concentration–discharge relationship for a wider range of vertical soil nitrate distribution and soil drainage parameters.

Figure 8a,b represents the enrichment stage and dilution stage, respectively. In each scenario, for a given K_{sat0} and N_{decay} , the corresponding 'slope' or general trend of concentration–discharge is computed for the enrichment stage (where the slope is positive) and the dilution stage (where the slope is negative). The enrichment stage in Figure 8a corresponds to the enrichment stage in Figure 7a–c, where the watershed is 'wetting up' and lateral flow from upslope would replenish nitrate, contributing to an enrichment concentration–discharge pattern (conceptual model Figure 4). The dilution stage in Figure 8b represents the dilution stage in Figure 7, where fast flow path or overland flow significantly increases the runoff with no additional nitrate replenishment, resulting in a dilution pattern.

In Figure 8a, higher N_{decay} (red and yellow dots) leads to steeper slope of the regression line (larger value in slopes), representing stronger enrichment. This is similar to results from our conceptual and numerical models for the patch scale. In Figure 8b, although the slopes of 'concentrated near surface' scenarios (red and yellow dots) are higher (less negative) than that of 'evenly distributed' scenarios (blue and black dots), the difference is small (~ 0.1) compared with the differences associated nitrate distribution in the enrichment stage in Figure 8a (~ 0.8). The lower sensitivity to vertical nitrate distribution in the dilution stage occurs because once the dilution state has been reached, most of the nitrate has been exported (during the 'enrichment' stage) and the nitrate reservoir exhausted. Low total nitrate means that the soil nitrate distribution has a much smaller impact on nitrate export. Nevertheless, in Figure 8b, the slope become larger in absolute value and the variance of slope across N_{decay} gets widened with higher hydraulic conductivity, showing that under higher hydraulic conductivity, the more evenly distributed nitrate cases will result in the stronger dilution relationship. Higher hydraulic conductivity and more evenly distributed nitrate will exhaust the soil nitrate reservoir faster than cases with lower hydraulic conductivity and less evenly distributed nitrate. If soil nitrate is more evenly distributed, more nitrate is allocated to middle or lower soil layers than the less evenly distributed cases, and more nitrate in the lower layers will be exported to downstream with a rising water table. When water table reaches the top layer and creates saturated area in near-stream riparian zone ('dilution' stage in Figure 8b), less nitrate will be left and the nitrate concentration will be lower in the more evenly distributed nitrate cases, resulting a stronger dilution relationship.

5 | DISCUSSION

This study focuses on the implications of the interactions between the vertical distribution of soil nitrate and hydraulic properties on nitrate concentration–discharge relationships at both patch and watershed scales. When soil nitrate and hydraulic conductivity decrease with depth, as is often the case, even a small difference in the rate of decay in either can lead to substantial differences in concentration–discharge patterns. These differences can include shifting between dilution and enrichment patterns. This sensitivity of model estimates of concentration–discharge patterns to the vertical distribution of soil nitrate and conductivity occurs at both patch and watershed scales, although responses are more complex at watershed scales due to the subsurface lateral nitrate replenishment from upslope areas.

Previous studies have stated that various factors control downstream nitrate concentration, such as nitrate source and hydrologic connectivity (Creed & Band, 1998a, 1998b), different land uses or land covers (Groffman, Williams, Pouyat, Band, & Yesilonis, 2009) and interactions of groundwater and nitrogen processes in the riparian zone (Duncan, Band, Groffman, & Bernhardt, 2015). For our semi-arid catchment, model estimates have a concentration discharge pattern of enrichment followed by dilution with increasing runoff. This pattern is consistent with the 'flushing' hypothesis (Creed & Band, 1998a, 1998b; Weiler & McDonnell, 2006), and with the observed concentration–discharge relationship for this site. To explain this pattern, previous hypotheses or conceptual models (such as 'nitrate flushing' hypotheses) argue that enrichment occurs with the expansion of the spatial extent of saturated area (variable source area) that connects previously disconnected nitrate rich locations. Dilution subsequently occurs when these locations become depleted of nitrate (Creed et al., 1996; Creed & Band, 1998a, 1998b). While our analysis provides a similar explanation for nitrate enrichment and dilution patterns, our model focuses on the vertical dimension, specifically the impact of how soil nitrate mass is distributed in a vertical soil profile relative to soil drainage properties. Our findings are consistent with the 'nitrate flushing' hypothesis but focuses on the relative *rate of change* in soil nitrate distribution in the vertical dimension, together with the *rate of change* in how soil releases water across its vertical profile. For our semi-arid study site, our model experiment demonstrates how these vertical properties can strongly shape: the steepness of the slope of runoff vs nitrate concentration curve during the enrichment phase, the threshold runoff at which concentration–discharge transitions to dilution and the steepness of the slope of the runoff vs nitrate concentration during the dilution phase.

Our results point to the importance of the underlying biological processes and geophysical properties that determine the vertical profiles of nitrate and hydraulic conductivity. Biological properties including plant species and their rooting distribution influence vertical nitrate distribution through N uptake (Kristensen & Thorup-Kristensen, 2007; McMurtrie et al., 2012; Soethe, Lehmann, & Engels, 2006). Vertical nitrate distributions also reflect the vertical

distribution of organic material and microbial processes that control substrate, mineralization and denitrification (Breland, 1994; Chen et al., 2017; Federer, 1983). Geophysical drainage properties that influence vertical redistribution of nitrate also play a role (Duncan et al., 2015; Schilling et al., 2007). Consequently spatial variation in plant species, subsurface biochemical composition and physical properties can combine to produce substantial spatial differences in vertical profiles of nitrate at plot to regional scales. These spatial patterns may give rise to spatial difference in nitrate concentration–discharge patterns.

While processes that influence vertical nitrate distribution were the dominant control on the concentration–discharge curve, patterns were also influenced by hydraulic conductivity profiles that reflect geophysical properties (Duncan et al., 2015; Weiler & McDonnell, 2006). We show that increasing the vertical divergence of nitrate mass (such that more nitrate is concentrated at surface) tends to steepen the enrichment of nitrate with increasing runoff. However this effect shows a non-linear relationship with hydraulic conductivity. For relatively low conductivity values, increasing conductivity also leads to a steeper enrichment slope. However, beyond a threshold conductivity (that varies with N_{decay}), higher conductivity reduces enrichment. Thus, greater drainage rates can intensify enrichment for relatively low runoff values. For example, for a watershed with a nitrate distribution characterized by strong N_{decay} with depth (>8), a difference in soil hydraulic conductivity from 5 to 50 would increase the enrichment slope from 0.9 to 1.2. Thus for two watersheds that differ only with respect to average drainage rates, the enrichment of N -concentration, as runoff increased from 1 to 10 mm/day, would be from a baseline concentration of 0.1 to 2.2 mg/L in the slower drainage (lower K case) but to 2.8 mg/L in a more rapidly draining watershed. The impact of hydraulic conductivity is a complex in that high drainage rates reduce the tendency toward steep enrichment behavior. While difference in the shape of the concentration–discharge curve with conductivity is less dramatic relative to the effect of differences in N_{decay} , the spatial heterogeneity in hydraulic conductivity and its decay with depth is often substantial (Figure 7). Vertical averaged conductivity and its distribution with depth can vary by several orders of magnitude with substrate properties and geomorphic evolutionary processes (Bray & Dunne, 2017; Landon, Rus, & Harvey, 2001).

5.1 | Application to other sites

In this model experiment with RHESSys, nitrate was assumed to decay exponentially with depth. Other distributions including non-monotonic increasing or decreasing functions may also occur and could be considered in future research. We focus on an exponential distribution since it likely reflects nitrate distribution in our semi-arid watershed (Goodridge & Melack, 2012; Parker & Schimel, 2011). Other distributions will likely produce both dilution and enrichment patterns, but relationships between nitrate-distribution parameters, hydraulic conductivity distribution parameters and concentration–discharge patterns will be different.

There are several processes that were not considered in this analysis, and which may also influence the concentration discharge patterns. Although we allowed the amount of nitrate to vary seasonally, with seasonal variation in vegetation update, immobilization and mineralization rates (Hanan et al., 2016b), we assumed that the vertical distribution of nitrate with depth does not change. In these steep semi-arid watersheds, fluxes associated with high runoff event may contribute additional nitrate and extend enrichment to higher flows, particularly for years following fire (Sherson, Van Horn, Gomez-Velez, Crossey, & Dahm, 2015). Future work will explore this additional complexity.

To some extent our results reflect behaviors that are linked to the strong seasonality of rainfall and biological processes found in semi-arid Mediterranean watersheds. In Figure 8a,b, the 'dilution' stage in the watershed scale simulation results requires a rapid increase in the volume of water in fast flowpaths including overland flow concurrent with limited nitrate replenishment. In Rattlesnake Creek watershed this scenario reflects relatively low rates of nitrate dry deposition and low rates of winter mineralization (Hanan et al., 2016b), when high runoff rates occur. In more humid areas or irrigated cropland, soil nitrate may accumulate at deeper soil depths (>1.3 m) (Benbi, Biswas, & Kalkat, 1991; Zhou, Gu, Schlesinger, & Ju, 2016) and have a smaller N decay rate. The smaller N -decay may reduce the slope of concentration discharge curve during the enrichment period (Figures 7 and 8), but additional simulation would be needed to include the influence of other controls on N availability and drainage.

6 | CONCLUSION

In this study, we proposed a conceptual model, which uses vertical soil nitrate distribution and its interaction with soil hydraulic conductivity to explain the nitrate concentration–discharge relationships. We designed a model experiment using an ecohydrologic model, RHESSys, applied to a semi-arid watershed, to show how concentration–discharge patterns may respond to soil vertical nitrate distribution and soil hydraulic conductivity, at both patch and watershed scales. Our findings are consistent with the nitrate-flushing hypothesis but add insight into how vertical biological and geophysical mediated properties can influence concentration–discharge patterns. In particular, we find that the vertical distribution of nitrate strongly influences the slope of the discharge concentration curve during the enrichment and dilution phases, and the runoff threshold where the transition between enrichment and dilution occurs. This sensitivity may contribute to mechanistic explanations for between watershed variations in concentration–discharge patterns, even in cases where topographic and climate controls lead to similar spatial patterns of runoff production. Future studies will expand this conceptual model and model experiments to account for a range of biogeoclimatic settings and explore both long- and short-term responses.

ACKNOWLEDGEMENT

Authors of this study thank the National Science Foundation for providing funding via the Santa Barbara Coastal Long Term Ecological Research Project (OCE-1458845 and SBC-LTER OCE-1232779).

DATA AVAILABILITY STATEMENT

The data (precipitation, water quality and streamflow data) that support the findings of this study are openly available in [hydrology and meteorology folder] at <http://sbc.lternet.edu//data/dataCollectionsPortal.html>.

ORCID

Xiaoli Chen  <https://orcid.org/0000-0002-0443-1372>

Christina L. Tague  <https://orcid.org/0000-0003-1463-308X>

REFERENCES

- Aguilera, R. and J.M. Melack. (2018a) Concentration-discharge responses to storm events in coastal California watersheds. *Water Resources Research*, 54:407–424. doi.org/10.1002/2017WR021578
- Aguilera, R., & Melack, J. M. (2018b). Relationships among nutrient and sediment fluxes, hydrological variability, fire, and land cover in coastal California catchments. *Journal of Geophysical Research – Biogeosciences*, 123(8), 2568–2589. <https://doi.org/10.1029/2017JG004119>
- Ameli, A. A., McDonnell, J. J., & Bishop, K. (2016). The exponential decline in saturated hydraulic conductivity with depth: A novel method for exploring its effect on water flow paths and transit time distribution. *Hydrological Processes*, 30, 2438–2450. <https://doi.org/10.1002/hyp.10777>
- Benbi, D. K., Biswas, C. R., & Kalkat, J. S. (1991). Nitrate distribution and accumulation in an ustochrept soil profile in a long term fertilizer experiment. *Fertilizer Research*, 28(2), 173–177. <https://doi.org/10.1007/BF01049747>
- Beven, K. J., & Kirkby, M. J. (1979). A physically based, variable contributing area model of basin hydrology/Un modèle à base physique de zone d'appel variable de l'hydrologie du bassin versant. *Hydrological Sciences Bulletin*, 24(1), 43–69. <https://doi.org/10.1080/02626667909491834>
- Beven, K., & Germann, P. (1982). Macropores and water flow in soils. *Water Resources Research*, 18(5), 1311–1325. <https://doi.org/10.1029/WR018i005p01311>
- Bowes, M. J., Jarvie, H. P., Halliday, S. J., Skeffington, R. A., Wade, A. J., Loewenthal, M., ... Palmer-Felgate, E. J. (2015). Characterising phosphorus and nitrate inputs to a rural river using high-frequency concentration-flow relationships. *Science of the Total Environment*, 511, 608–620. <https://doi.org/10.1016/j.scitotenv.2014.12.086>
- Bray, E. N., & Dunne, T. (2017). Subsurface flow in lowland river gravel bars. *Water Resources Research*, 53(9), 7773–7797. <https://doi.org/10.1002/2016WR019514>
- Breland, T. A. (1994). Enhanced mineralization and denitrification as a result of heterogeneous distribution of clover residues in soil. *Plant and Soil*, 166(1), 1–12.
- Chen, J., Xiao, G., Kuzyakov, Y., Jenerette, G. D., Ma, Y., Liu, W., ... Shen, W. (2017). Soil nitrogen transformation responses to seasonal precipitation changes are regulated by changes in functional microbial abundance in a subtropical forest. *Biogeosciences*, 14(9), 2513–2525. <https://doi.org/10.5194/bg-14-2513-2017>
- Creed, I. F., & Band, L. E. (1998a). Exploring functional similarity in the export of nitrate-N from forested catchments: A mechanistic modeling approach. *Water Resources Research*, 34(11), 3079–3093. <https://doi.org/10.1029/98wr02102>
- Creed, I. F., & Band, L. E. (1998b). Export of nitrogen from catchments within a temperate forest: Evidence for a unifying mechanism regulated by variable source area dynamics. *Water Resources Research*, 34(11), 3105–3120. <https://doi.org/10.1029/98wr01924>
- Creed, I. F., Band, L. E., Foster, N. W., Morrison, I. K., Nicolson, J. A., Semkin, R. S., & Jeffries, D. S. (1996). Regulation of nitrate-N release from temperate forests: A test of the N flushing hypothesis. *Water Resources Research*, 32(11), 3337–3354. <https://doi.org/10.1029/96wr02399>
- Demenico, P. A., & Schwartz, F. W. (1990). *Physical and chemical hydrogeology*. New York, NY 10158-0012: John Wiley and Sons, Inc.
- Duncan, J. M., Band, L. E., Groffman, P. M., & Bernhardt, E. S. (2015). Mechanisms driving the seasonality of catchment scale nitrate export: Evidence for riparian ecohydrologic controls. *Water Resources Research*, 51(6), 3982–3997. <https://doi.org/10.1002/2015WR016937>
- Federer, C. A. (1983). Nitrogen mineralization and nitrification: depth variation in four New England forest soils. *Soil Science Society of America Journal*, 47(5), 1008–1014. <https://doi.org/10.2136/sssaj1983.03615995004700050034x>
- Freer, J., McDonnell, J. J., Beven, K. J., Peters, N. E., Burns, D. A., Hooper, R. P., ... Kendall, C. (2002). The role of bedrock topography on subsurface storm flow. *Water Resources Research*, 38(12), 5-1–5-16. <https://doi.org/10.1029/2001WR000872>
- Galloway, J. N., Aber, J. D., Erisman, J. W., Seitzinger, S. P., Howarth, R. W., Cowling, E. B., & Cosby, B. J. (2003). The nitrogen cascade. *BioScience*, 53(4), 341–356. [https://doi.org/10.1641/0006-3568\(2003\)053\[0341:tnc\]2.0.co;2](https://doi.org/10.1641/0006-3568(2003)053[0341:tnc]2.0.co;2)
- Godsey, S. E., Kirchner, J. W., & Clow, D. W. (2009). Concentration-discharge relationships reflect chemostatic characteristics of US catchments. *Hydrological Processes*, 23(13), 1844–1864. <https://doi.org/10.1002/hyp.7315>
- Goodridge, B. M., Hanan, E. J., Aguilera, R., Wetherley, E. B., Chen, Y.-J., D'Antonio, C. M., & Melack, J. M. (2018). Retention of nitrogen following wildfire in a chaparral ecosystem. *Ecosystems*, 21(8), 1608. <https://doi.org/10.1007/s10021-018-0243-3>
- Goodridge, B.M., & Melack, J. M. (2012). Land use control of stream nitrate concentrations in mountainous coastal California watersheds. *Journal of Geophysical Research – Biogeosciences*, 117(G2), G02005. doi: <https://doi.org/10.1029/2011JG001833>
- Graham, C. B., Woods, R. A., & McDonnell, J. J. (2010). Hillslope threshold response to rainfall: (1) A field based forensic approach. *Journal of Hydrology*, 393(1), 65–76. <https://doi.org/10.1016/j.jhydrol.2009.12.015>
- Green, W., & Ampt, G. A. (1911). Studies on soil physics. *The Journal of Agricultural Science*, 4(1), 1–24. <https://doi.org/10.1017/S0021859600001441>
- Groffman, P. M., Williams, C. O., Pouyat, R. V., Band, L. E., & Yesilonis, I. D. (2009). Nitrate leaching and nitrous oxide flux in urban forests and Grasslands. *Journal of Environmental Quality*, 38(5), 1848–1860. <https://doi.org/10.2134/jeq2008.0521>
- Hanan, E. J., D'Antonio, C. M., Roberts, D. A., & Schimel, J. P. (2016a). Factors regulating nitrogen retention during the early stages of recovery from fire in Coastal Chaparral ecosystems. *Ecosystems*, 19(5), 910–926. <https://doi.org/10.1007/s10021-016-9975-0>
- Hanan, E. J., Tague, C., & Schimel, J. P. (2016b). Nitrogen cycling and export in California chaparral: The role of climate in shaping ecosystem responses to fire. *Ecological Monographs*, 87(1), 76–90. <https://doi.org/10.1002/ecm.1234>
- Harms, T. K., & Grimm, N. B. (2010). Influence of the hydrologic regime on resource availability in a semi-arid stream-riparian corridor. *Ecohydrology*, 3(3), 349–359. <https://doi.org/10.1002/eco.119>
- Hedin, L. O., Armesto, J. J., & Johnson, A. H. (1995). Patterns of nutrient loss from unpolluted, old-growth temperate forests: Evaluation of biogeochemical theory. *Ecology*, 76(2), 493–509. <https://doi.org/10.2307/1941208>
- Homyak, P. M., Sickman, J. O., Miller, A. E., Melack, J. M., Meixner, T., & Schimel, J. P. (2014). Assessing nitrogen-saturation in a seasonally dry chaparral watershed: Limitations of traditional indicators of N-saturation. *Ecosystems*, 17, 1–20. <https://doi.org/10.1007/s10021-014-9792-2>
- Hornberger, G. M., Bencala, K. E., & McKnight, D. M. (1994). Hydrological controls on dissolved organic-carbon during snowmelt in the snake river near Montezuma, Colorado. *Biogeochemistry*, 25(3), 147–165. <https://doi.org/10.1007/bf00024390>
- House, W. A., & Warwick, M. S. (1998). Hysteresis of the solute concentration/discharge relationship in rivers during storms. *Water*

- Research, 32(8), 2279–2290. [https://doi.org/10.1016/S0043-1354\(97\)00473-9](https://doi.org/10.1016/S0043-1354(97)00473-9)
- Jencso, Kelsey G., McGlynn, Brian L., Gooseff, Michael N., Bencala, Kenneth E., & Wondzell, Steven M. (2010). Hillslope hydrologic connectivity controls riparian groundwater turnover: Implications of catchment structure for riparian buffering and stream water sources. *Water Resources Research*, 46(10), W10524. doi: <https://doi.org/10.1029/2009WR008818>
- Jiang, R., Hatano, R., Hill, R., Kuramochi, K., Jiang, T., & Zhao, Y. (2015). Water connectivity in hillslope of upland-riparian zone and the implication for stream nitrate-N export during rain events in an agricultural and forested watershed. *Environmental Earth Sciences*, 74(5), 4535–4547. <https://doi.org/10.1007/s12665-015-4516-2>
- Kothawala, D. N., & Moore, T. R. (2009). Adsorption of dissolved nitrogen by forest mineral soils. *Canadian Journal of Forest Research*, 39(12), 2381–2390. <https://doi.org/10.1139/X09-147>
- Kristensen, H. L., & Thorup-Kristensen, K. (2007). Effects of vertical distribution of soil inorganic nitrogen on root growth and subsequent nitrogen uptake by field vegetable crops. *Soil Use and Management*, 23(4), 338–347. <https://doi.org/10.1111/j.1475-2743.2007.00105.x>
- Landon, M. K., Rus, D. L., & Harvey, F. E. (2001). Comparison of instream methods for measuring hydraulic conductivity in sandy streambeds. *Groundwater*, 39(6), 870–885. <https://doi.org/10.1111/j.1745-6584.2001.tb02475.x>
- Lohse, K. A., Sanderman, J., & Amundson, R. (2013). Identifying sources and processes influencing nitrogen export to a small stream using dual isotopes of nitrate. *Water Resources Research*, 49(9), 5715–5731. <https://doi.org/10.1002/wrcr.20439>
- López-Moreno, J. I., Zabalza, J., Vicente-Serrano, S. M., Revuelto, J., Gilaberte, M., Azorin-Molina, C., ... Tague, C. (2014). Impact of climate and land use change on water availability and reservoir management: Scenarios in the Upper Aragón River, Spanish Pyrenees. *Science of the Total Environment*, 493(0), 1222–1231. <https://doi.org/10.1016/j.scitotenv.2013.09.031>
- Macrae, M. L., English, M. C., Schiff, S. L., & Stone, M. (2010). Influence of antecedent hydrologic conditions on patterns of hydrochemical export from a first-order agricultural watershed in Southern Ontario, Canada. *Journal of Hydrology*, 389(1–2), 101–110. doi: <https://doi.org/10.1016/j.jhydrol.2010.05.034>
- McDonnell, J. J. (1990). A rationale for old water discharge through macropores in a steep, humid catchment. *Water Resources Research*, 26(11), 2821–2832. <https://doi.org/10.1029/WR026i011p02821>
- McMurtrie, R. E., Iversen, C. M., Dewar, R. C., Medlyn, B. E., Näsholm, T., Pepper, D. A., & Norby, R. J. (2012). Plant root distributions and nitrogen uptake predicted by a hypothesis of optimal root foraging. *Ecology and Evolution*, 2(6), 1235–1250. <https://doi.org/10.1002/ece3.266>
- Meixner, T., Huth, A. K., Brooks, P. D., Conklin, M. H., Grimm, N. B., Bales, R. C., ... Petti, J. R. (2007). Influence of shifting flow paths on nitrogen concentrations during monsoon floods, San Pedro River, Arizona. *Journal of Geophysical Research - Biogeosciences*, 112(3), G03S03. <https://doi.org/10.1029/2006JG000266>
- Melack, J. M. (2010). SBC LTER: Land: Hydrology: Santa Barbara County Flood Control District - Precipitation at El Deseo (ElDeseo255). Santa Barbara Coastal LTER. knb-lter-sbc.5008.5. (<http://metacat.lternet.edu/knb/metacat/knb-lter-sbc.5008.5/lter>)
- Melack, J. M. (2012a). SBC LTER: Land: Hydrology: Stream discharge and associated parameters at Rattlesnake Creek, Las Canoas Rd (RS02). Santa Barbara Coastal LTER. knb-lter-sbc.3013.6 (<http://metacat.lternet.edu/knb/metacat/knb-lter-sbc.3013.6/lter>)
- Melack, J. M. (2012b). SBC LTER: Land: Stream chemistry in the Santa Barbara Coastal drainage area. Santa Barbara Coastal LTER. knb-lter-sbc.6.13 (<http://metacat.lternet.edu/knb/metacat/knb-lter-sbc.6.13/lter>)
- Miller, A. E., Schimel, J. P., Meixner, T., Sickman, J. O., & Melack, J. M. (2005). Episodic rewetting enhances carbon and nitrogen release from chaparral soils. *Soil Biology & Biochemistry*, 37(12), 2195–2204. <https://doi.org/10.1016/j.soilbio.2005.03.021>
- Monteith, J. L. (1965). Evaporation and the environment. *The State and Movement of Water in Living Organisms*, 19, 205–234.
- Nash, J. E., & Sutcliffe, J. V. (1970). River flow forecasting through conceptual models part I – A discussion of principles. *Journal of Hydrology*, 10(3), 282–290. [https://doi.org/10.1016/0022-1694\(70\)90255-6](https://doi.org/10.1016/0022-1694(70)90255-6)
- Ocampo, C. J., Oldham, C. E., Sivapalan, M., & Turner, J. V. (2006). Hydrological versus biogeochemical controls on catchment nitrate export: a test of the flushing mechanism. *Hydrological Processes*, 20(20), 4269–4286. <https://doi.org/10.1002/hyp.6311>
- Page, H. M., Reed, D. C., Brzezinski, M. A., Melack, J. M., & Dugan, J. E. (2008). Assessing the importance of land and marine sources of organic matter to kelp forest food webs. *Marine Ecology Progress Series*, 360, 47–62.
- Parker, S. S., & Schimel, J. P. (2011). Soil nitrogen availability and transformations differ between the summer and the growing season in a California grassland. *Applied Soil Ecology*, 48(2), 185–192. <https://doi.org/10.1016/j.apsoil.2011.03.007>
- Parton, W. J., Mosier, A. R., Ojima, D. S., Valentine, D. W., Schimel, D. S., Weier, K., & Kulmala, A. E. (1996). Generalized model for N₂ and N₂O production from nitrification and denitrification. *Global Biogeochemical Cycles*, 10(3), 401–412. <https://doi.org/10.1029/96GB01455>
- Peters, D. L., Buttle, J. M., Taylor, C. H., & Lazerte, B. D. (1995). Runoff production in a forested, shallow soil, Canadian Shield Basin. *Water Resources Research*, 31(5), 1291–1304. <https://doi.org/10.1029/94wr03286>
- Philip, J. R. (1957). The theory of infiltration: 4. Sorptivity and algebraic infiltration equations. *Soil Science*, 84(3) 257–264. <https://doi.org/10.1097/00010694-195709000-00010>
- Rundel, P. W. (1982). Nitrogen utilization efficiencies in mediterranean-climate shrubs of California and Chile. *Oecologia*, 55(3), 409–413. <https://doi.org/10.1007/BF00376930>
- Schilling, K. E., Tomer, M. D., Zhang, Y. K., Weisbrod, T., Jacobson, P., & Cambardella, C. A. (2007). Hydrogeologic controls on nitrate transport in a small agricultural catchment, Iowa. *Journal of Geophysical Research - Biogeosciences*, 112(G3), G03007. <https://doi.org/10.1029/2007JG000405>
- Schlesinger, W. H. (1985). Decomposition of Chaparral shrub foliage. *Ecology*, 66(4), 1353–1359. <https://doi.org/10.2307/1939188>
- Sherson, L. R., Van Horn, D. J., Gomez-Velez, J. D., Crossey, L. J., & Dahm, C. N. (2015). Nutrient dynamics in an alpine headwater stream: use of continuous water quality sensors to examine responses to wild-fire and precipitation events. *Hydrological Processes*, 29(14), 3193–3207. <https://doi.org/10.1002/hyp.10426>
- Shields, C., & Tague, C. (2012). Assessing the role of parameter and input uncertainty in ecohydrologic modeling: Implications for a semi-arid and urbanizing coastal California catchment. *Ecosystems*, 15(5), 775–791. <https://doi.org/10.1007/s10021-012-9545-z>
- Soethe, N., Lehmann, J., & Engels, C. (2006). The vertical pattern of rooting and nutrient uptake at different altitudes of a south Ecuadorian Montane forest. *Plant and Soil*, 286, 287. <https://doi.org/10.1007/s11104-006-9044-0>
- Swarowsky, A., Dahlgren, R. A., & O'Geen, A. T. (2012). Linking subsurface lateral flowpath activity with streamflow characteristics in a semiarid headwater catchment. *Soil Science Society of America Journal*, 76(2), 532–547. <https://doi.org/10.2136/sssaj2011.0061>
- Tague, C. L., & Band, L. E. (2004). RHESys: Regional hydro-ecologic simulation system-an object-oriented approach to spatially distributed modeling of carbon, water, and nutrient cycling. *Earth Interactions*, 8, 1–42. [https://doi.org/10.1175/1087-3562\(2004\)8<1:RRHSSO>2.0.CO;2](https://doi.org/10.1175/1087-3562(2004)8<1:RRHSSO>2.0.CO;2)
- Tague, C., Seaby, L., & Hope, A. (2009). Modeling the eco-hydrologic response of a Mediterranean type ecosystem to the combined impacts of projected climate change and altered fire frequencies. *Climatic*

- Change, 93(1–2), 137–155. <https://doi.org/10.1007/s10584-008-9497-7>
- Thornton, Peter E. (1998). *Regional ecosystem simulation: combining surface- and satellite-based observations to study linkages between terrestrial energy and mass budgets*. (Ph.D. dissertation), University of Montana, Missoula MT.
- Weiler, M., & McDonnell, J. J. (2006). Testing nutrient flushing hypotheses at the hillslope scale: A virtual experiment approach. *Journal of Hydrology*, 319(1), 339–356. <https://doi.org/10.1016/j.jhydrol.2005.06.040>
- Zhou, Junyu, Gu, Baojing, Schlesinger, William H., & Ju, Xiaotang. (2016). Significant accumulation of nitrate in Chinese semi-humid croplands. *Scientific Reports*, 6, 25088. doi: <https://doi.org/10.1038/srep25088> <http://www.nature.com/articles/srep25088> - supplementary-information
- Zimmer, M. A., Pellerin, B., Burns, D. A., & Petrochenkov, G. (2019). Temporal variability in nitrate-discharge relationships in large rivers as revealed by high-frequency data. *Water Resources Research*, 55(0), 973–989. <https://doi.org/10.1029/2018WR023478>

How to cite this article: Chen X, Tague CL, Melack JM, Keller AA. Sensitivity of nitrate concentration-discharge patterns to soil nitrate distribution and drainage properties in the vertical dimension. *Hydrological Processes*. 2020;34: 2477–2493. <https://doi.org/10.1002/hyp.13742>